MOTION REALIZATION OF A SMALL DIAMETER DEEP WELL RESCUE ROBOT BASED ON ADAMS-MATLAB CO-SIMULATION

Yi Zheng[1], Jixin Liu[1], Maohua Xiao[2]**
[1]Institute of Intelligence and Manufacture, Qingdao Huanghai University, Qingdao, 266427, China;
[2]College of Engineering, Nanjing Agricultural University, Nanjing 210031, China;
zhengy@qdhhc.edu.cn, xiaomaohua@njau.edu.cn , fw.2004@163.com;
**Correspondence: xiaomaohua@njau.edu.cn*

Abstract: A small diameter deep well rescue robot is proposed in this work to address issues including special well conditions and the difficulty of small diameter deep well rescue. In order to achieve efficient rescue, combined with small diameter deep wells, establish an efficient smart small caliber deep well rescue robot. A virtual prototype model of the mechanism is established using the 3D design software SOLIDWORKS. Based on the principle of PD automatic control, the joint control of ADAMS and MATLAB is carried out. The control function of each driver is set, along with the input and output variables, and a joint control file is generated. The PD automatic control code is compiled in MATLAB software, and a Simulink simulation control block diagram is designed. The entire rescue process is then simulated, and the change track of the output variable is obtained. The results show that the rescue robot can detect the position of a person who has fallen into a well. By rotating the manipulator, the robot can reach the ideal grasping position. Facilitated by the grasp of the manipulator and the secondary protection of the bracket mechanism, the rescue robot can then complete the deep well rescue work.

Keywords: Small caliber; Deep well rescue robot; Joint control; Motion realization.

1. Introduction

There are a large number of mines, pile shaft, motor-pumped wells and irrigation in the rural areas of our country, and also some tube wells laid for water supply, drainage, gas and electric power in the urban construction [1-2]. Most of these wells are in the open air, virtually formed a hidden security problem [3]. China has a great number of such accidents every year. Due to the small caliber of these wells, most of them only 30 to 100 cm range. There is no special rescue equipment so that it's very difficult and takes long time to make aid work [4-5], sometimes 10 hours, or even longer, resulting in people injured seriously and even death for the trapped treatment is not promptly.

With regard to this work, a deep well rescue robot was developed and designed to retrieve persons falling into a well [6]. An increasing amount of pipeline wells for water supply, drainage, gas, electricity, etc., are being constructed due to the development of industry and urban construction. Due to a lack of proper management, some pipeline wells in rural areas, including some dry wells and field irrigation wells, are also in the open air, while construction site wells are often not filled in time after being used [7-10]. As individuals are often not aware of the precautions to take around pipeline wells, this phenomenon presents a safety risk to human lives [11-13].

In view of the complexity and special nature of the rescue site of the small diameter deep well, a multi- function deep well rescue robot is designed [14-16]. The robot consists of a well supporting part, a traveling mechanism, a crawler arm, anchor mechanism, and auxiliary system, including lighting, imaging, location sensing, and the like. Considering the different postures of falling porters, the rescue robot arm needs to adjust the grab position according to the situation to get the best rescue direction [17-20].

2. A Small-caliber Deep Well Rescue Robot Prototype Model

The designed small-caliber deep well rescue robot mainly consists of a body, a fixed mechanism, a traveling mechanism, a bracket mechanism, a mechanical arm guide rail, a grasping mechanism, and accessory devices. The accessory devices predominantly include lighting, camera, and sensing devices. When a fall accident occurs, the small-caliber deep well rescue robot will enter the well through a traveling mode of suspension and walking mechanisms. When the distance sensor at the bottom of the body detects the distance till stopping, it will send a signal to halt the progression to the driving mechanism, which will stop the robot. The sensor fusion system detects the conditions at the bottom of the well, including humidity, temperature, CO, oxygen content, methane, and other harmful gases, providing information for rescuers to develop a rescue plan. The prototype model of the proposed small-diameter deep well rescue robot is shown in Figure 1.

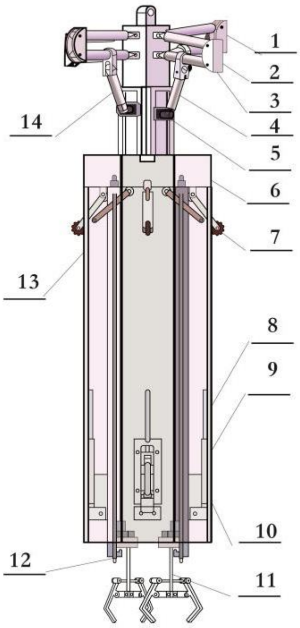

1. Fixed block;
2. Fixed support rod;
3. Fixed sleeve;
4. Fixed link;
5. Push block (connected with linear motor);
6. Body;
7. Marching agency;
8. Carriage slide rail (connected to the drive);
9. Bracket mechanism;
10. Robotic arm guide;
11 Grabbing mechanism (linear motor drive);
12. Sensor system;
13. Lighting and camera system

Figure 1: A small-caliber deep well rescue robot

The position of the robot's grasping mechanism is adjusted according to the posture of the person in the well. The tray of the stand mechanism is then opened to a vertical position to make room for the manipulator to move up and down. The rescue personnel can clearly see the movement of the downhole manipulator through the camera device and control it so that the manipulator's gripping mechanism can take hold of the person inside the well. The manipulator arm will then lift to move upwards.

When the position of the well falls to the top of the bracket mechanism, the bracket mechanism begins to rotate so that the pallet moves to the horizontal position to prevent the person from falling back to the bottom of the well. When the manipulator and the carriage mechanism reach the designated position, the lifting mechanism and the traveling mechanism move simultaneously to transport the robot to the well to realize deep well rescue.

This rescue process is denoted in Figure 2.

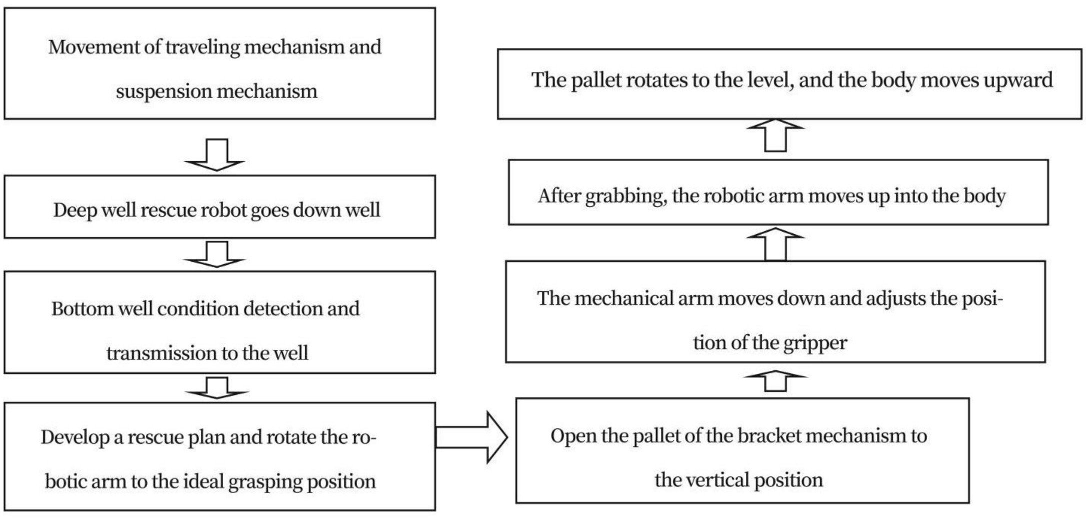

Figure 2: Rescue process

2.1 Marching Agency

The designed deep well rescue robot moves up and down in the well using two mechanisms: one is the hoisting mechanism on the well, which uses rollers and ropes to move the deep well rescue robot up and down in the well; the other uses rollers to move up and down along the inner wall of the well. The roller can not only roll up and down along the shaft wall but can also be fixed on the shaft wall at a certain place where it needs to be stopped, helping to maintain the stability of the deep well rescue robot.

The traveling mechanism design employs the principle of an aircraft landing gear and is shown in Figure 3.

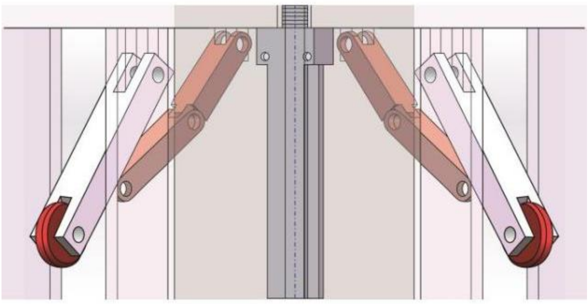

Figure 3: Schematic diagram of marching mechanism

The traveling mechanism is designed using the working principle of an aircraft landing gear. According to the circular shape of the well head, a traveling mechanism is designed at 90° intervals. When the traveling mechanism is fully opened, it has a self-locking function so that it can be stabilized at any position in the well. However, it is different from how the landing gear of an aircraft is mounted. When the walking mechanism of the deep well rescue robot is fully operational, the roller is not in a vertical state and instead maintains a certain angle with the well wall in order to better realize the fixation and facilitate the deployment of the clamping mechanism for rescue.

2.2 Grabbing Mechanism

The grasping mechanism is the execution mechanism of the rescue robot for deep wells. The shoulders, armpits, or waist of the individual being rescued are grasped by the gripping mechanism's claws, and they are lifted to the ground through the lifting mechanism. Thus, the role of the grasping mechanism is highly important and determines whether the person can be rescued successfully. The gripping force is also a key aspect of the design. The gripping mechanism is shown in Figure 4.

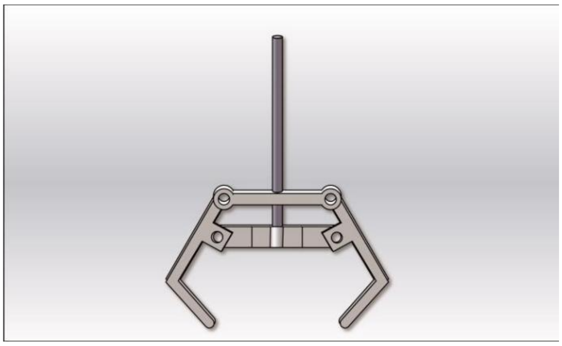

Figure 4: Schematic diagram of grasping mechanism

The grasping mechanism is the only component of the entire mechanical arm that performs the grasping action. After grasping the person inside the well, they must be lifted into the shell of the rescue robot when the body mechanism of the rescue robot is stationary. The hoisting mechanism uses a crank slider, and the sliding block is connected with the claw component to realize the rise and fall. The claw structure is connected to a linear motor which completes the opening and closing of the claw.

2.3 Bracket

After the claws grab the rescued person and rise into the rescue robot's shell, the bracket at the bottom of the rescue robot provides upward support for the person. This prevents the claws from gripping too tightly as well as the person from falling into the bottom of the well again. The bracket is designed with a crank-slider mechanism, and the movement is limited. Before the rescue, the bracket swings parallel to the shaft wall to allow the up and down movement of the open claw. When the claw grabs the person and rises to the bracket, the bracket flips to a horizontal position to support the individual and provide assistance for the claws. Since the rescue robot has a circular structure, there are a total of four brackets designed to be spaced 90° apart. The bracket structure is shown in Figure 5.

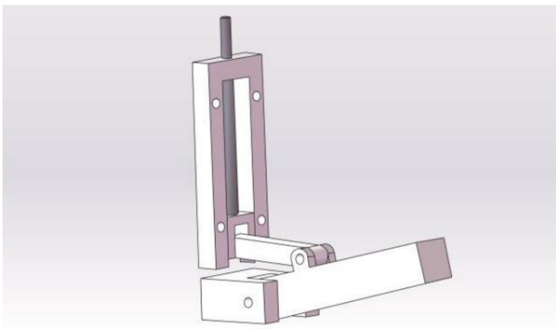

Figure 5: Bracket structure diagram

The connection between the bracket and the robot body is shown in Figure 6.

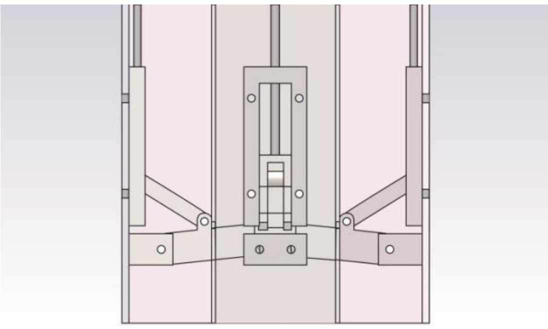

Figure 6 Schematic diagram of the connection between the bracket and the body

3. PD Automatic Control Principle

The PD controller exerts the proportional–derivative control law.

Features of the PD control mode:

A PD linear feedback controller is used in various independent motion joints. It is widely used in industrial robot control as it is easy to design and can ensure gradual stability.

The relationship between the output m(t) and input e(t) is shown in the following formula:

$$m(t) = K_p e(t) + K_p \tau \frac{de(t)}{dt}$$

where Kp is the proportional coefficient and τ is the differential time constant. Both Kp and τ are adjustable parameters. The PD controller is shown in Figure 7.

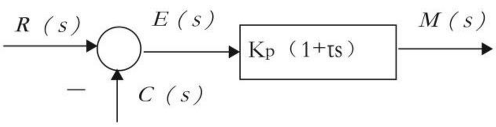

Figure 7: PD controller

During series calibration, an open-loop zero point of −1/τ can be added to the system to increase its phase angle margin, thus contributing to the improvement of the dynamic performance of the system. The differential control law in the PD controller can reflect the change trend of the input signal and generate an effective early correction signal to increase the damping degree of the system, thereby improving its stability.

4. Realization of Automatic Control Based on ADAMS and MATLAB

The control method of the deep well rescue robot is PD automatic control, which uses the difference between the target value and the initial value. The control mainly includes two aspects of the rescue robot body: moving downwards and upwards. Before grasping, the angle of the manipulator and the grasping target angle is adjusted.

4.1 Control Function

The STEP function is employed to define the up and down motion control function of the rescue robot body, the rotation control function before manipulator grabbing, and the control function of the manipulator grabbing.

(1) Up and down motion control function of rescue robot body

Taking the behavior of the rescue robot body as an example, the downward motion drive is named general_motion_1. The downward motion time is obtained according to the motion simulation, and the STEP control function of motion is obtained in the Z direction, as shown in Figure 8.

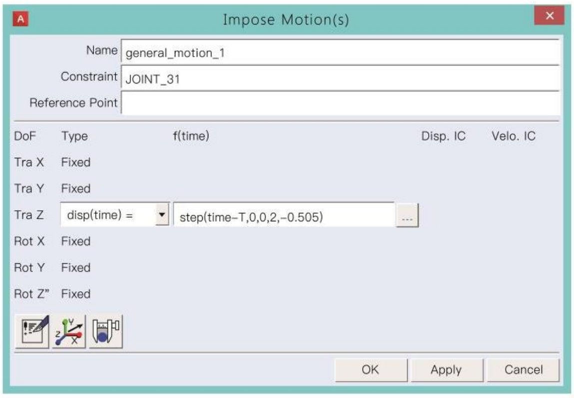

Figure 8: Downward motion control function of rescue robot body

(1) Grasping motion control function of rescue robot manipulator

According to the specific position of the falling target, the relative position of the robot arm is adjusted to facilitate grasping, and the motion drive of the robot grasp is formulated. This is named general_motion_2. The grasping motion time is obtained according to the motion simulation. The STEP control function of the movement in the Z direction is shown in Figure 9.

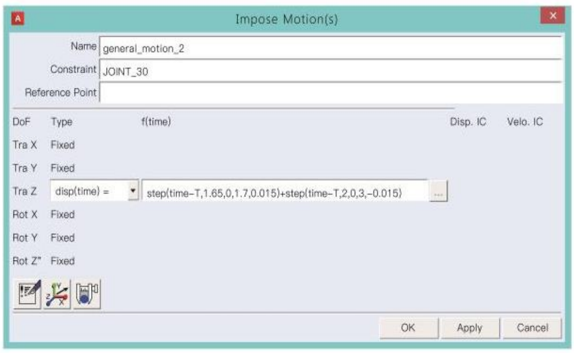

Figure 9: Grasping motion control function of rescue robot

(2) Rotational motion control function of rescue robot manipulator.

The relative position of the robot arm and the falling target is adjusted according to the specific position of the falling target. This rotation to a position aligned with the target formulates the motion drive of the robot rotation, which is named general_motion_3. The rotation motion time is obtained according to the motion simulation. Figure 10 shows the STEP control function of the movement in the Z direction.

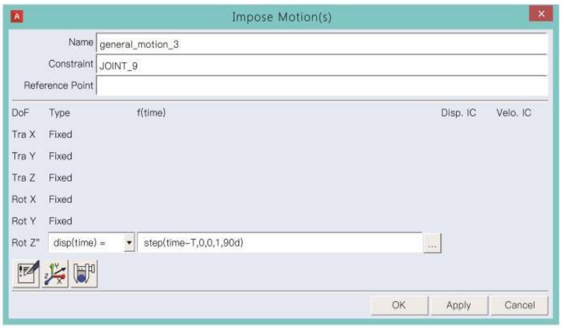

Figure 10: Rotational motion control function of rescue robot manipulator

4.2 Define State Variables

(1) The initial state variables of the rescue robot

OUT_Y0 is defined as the lowest point of the rescue robot body and the initial state variable of the rescue robot, as shown in Figure 11.

(2) Target variable

Taking the position of the center of the target mass as the target point, OUT_Y1 is defined as the falling target variable, as shown in Figure 12.

(3) The return of the rescue robot to the position variable after grabbing

After the rescue robot grabs the target in the well, it must return to the top of the well and define OUT_Y2 to return the target position variable, as shown in Figure 13.

(4) Variables of the angle between the falling well target and the robot body

When the rescue robot descends to the specified position, the angle between the manipulator and the falling target must be adjusted to facilitate grasping. Here, OUT_AG is defined as the angle variable between the two, as shown in Figure 14.

(5) Variables of driving force of rescue robot moving downwards

INT_F is defined as the driving force variable of the rescue robot's downward motion, as shown in Figure 15.

(6) Variables of driving force of rescue robot moving downwards

When there is an angle between the robot arm and the target, it cannot be grasped. Therefore, the angle of the robot arm must be adjusted, and INT_M is defined as the driving torque variable of the rescue robot arm rotation motion, as shown in Figure 16.

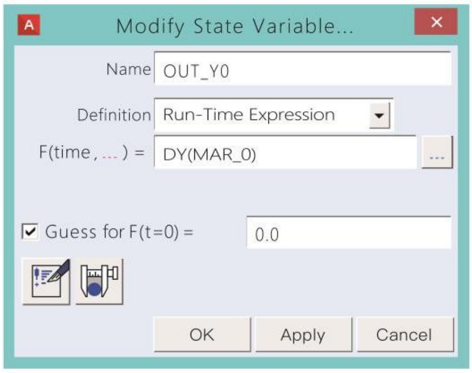

Figure 11: Definition of initial position variables of rescue robot

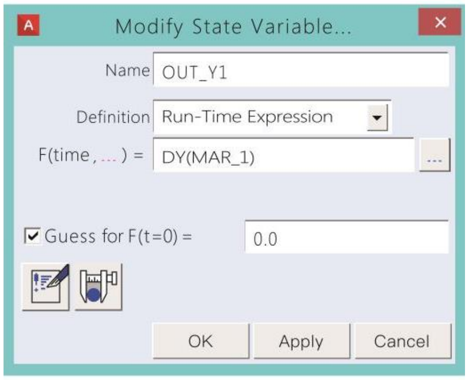

Figure 12: Definition of target variables

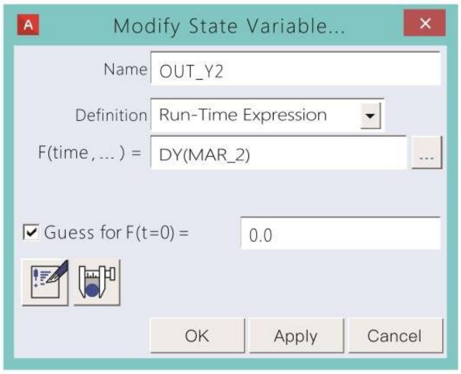

Figure 13: The rescue robot returns the target variable

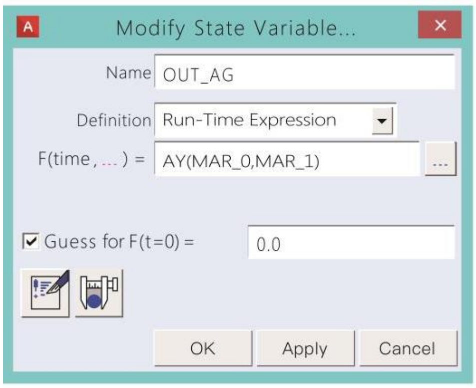

Figure 14: Target variable of the angle between the manipulator and the target

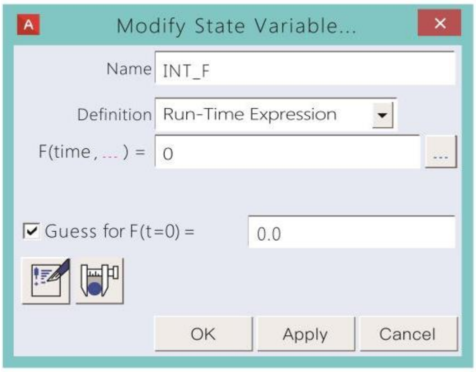

Figure 15: Driving force variable of rescue robot downward motion

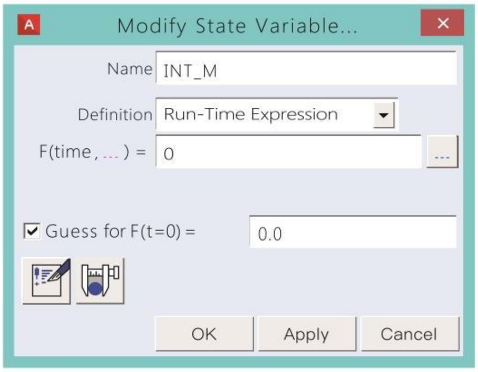

Figure 16: Variable of driving torque of manipulator rotation motion

The Simulink control block diagram was obtained in MATLAB software by entering adams_sys in the command window and pressing Enter. The final Simulink control block diagram after editing and sorting is shown in Figure 17.

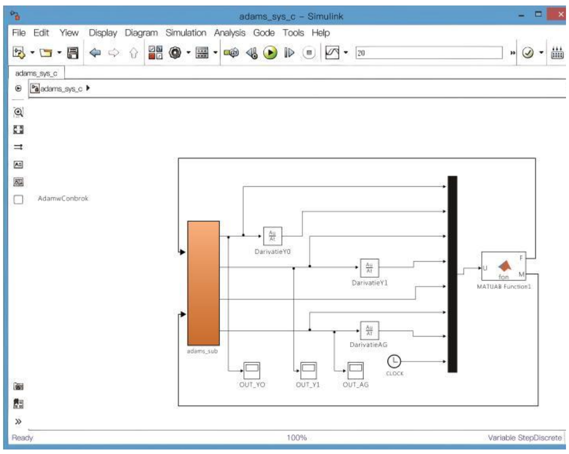

Figure 17: Simulink control block diagram

5. Motion Simulation

Based on MATLAB, the simulation time was set to 20 s, and a simulation was performed to obtain the change curve of each output variable.

The results are shown in Figures 18 and 19.

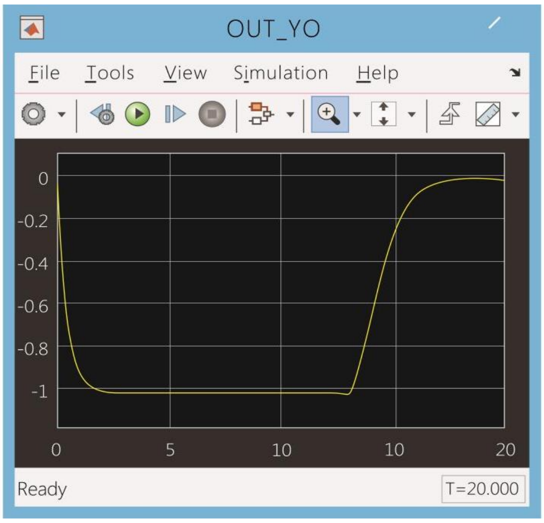

Figure 18: Rescue movement process of rescue robot body

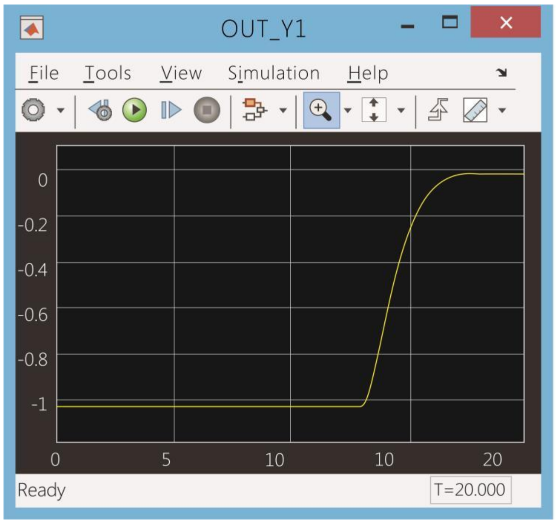

Figure 19: The movement process of the center of mass of the falling target

It can be seen from the simulation result graph in Figure 18 that the initial position is defined as the zero point. The rescue robot starts from the initial position and moves downwards. The distance between the calibration point of the robot body and the calibration point of the falling target is used to determine when the robot's downward movement will stop. Figure 19 shows the change curve of the center of the target mass. With the grasping movement and the ascent of the robot body, the center of the mass of the target reaches the initial position of the robot body at about 18 s, and well rescue is achieved.

After the simulation, the results are imported from ADAMS to view the data. The import process is shown in Figures 20 and 21.

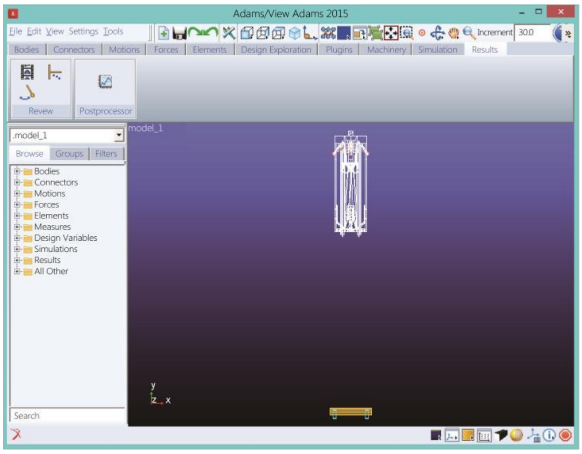

Figure 20: Rescue initial state

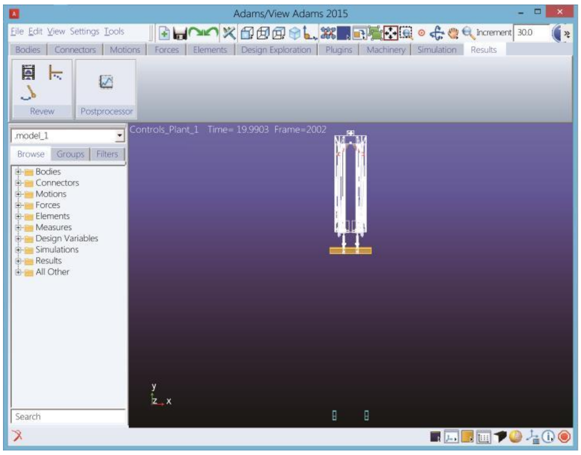

Figure 21: Rescue end state

ADAMS post-processing was used to view the simulation results. The resulting curve of the control force of the rescue robot's up and down movement is shown in Figure 22.

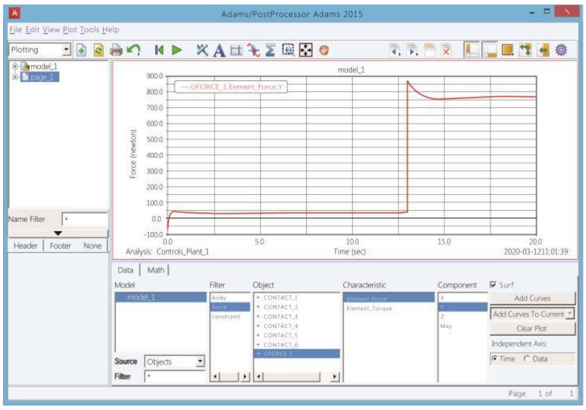

Figure 22: Change curve of driving force of rescue robot body movement

It can be seen from Figure 22 that when the rescue robot body descends, under the combined action of the suspension mechanism and the traveling mechanism, the force is small, which verifies that the lightweight optimization meets the requirements of use; when it runs to 13 s, the rescue robot completes its mission. In order to achieve the grasping action, it must move upwards. After increasing the weight of the feller, the grasping force is finally stabilized at 750 N, which can meet the requirements for use in small-caliber rescue robots. The change curve of gripping force is essentially the same as the expected change law, which can meet the needs of deep well rescue work.

6. Conclusions

This work explored the automatic control of rescue robots. Using PD automatic control theory and based on ADAMS-MATLAB joint control, the STEP control function of each motion module and the input and output variables were set in ADAMS, and the joint control file was formulated. MATLAB software was used to obtain the Simulink control block diagram, compile the PD automatic control code, simulate the movement process of the deep well rescue robot, and obtain the change curve of the output variables.

The simulation data results were verified in ADAMS, and the force and moment curves during the up and down movement of the deep well rescue robot were obtained to achieve precise control of the entire rescue process.

Acknowledgments

This work was supported by Shandong Key Research and Development Project (No.2019GHY112068), Qingdao postdoctoral applied research project (A2020-070、the Natural Science Foundation of Shandong Province (No.ZR2020QE151) and Qingdao Huanghai University doctoral research Fund Project (2020boshi02).

References

[1] Singh G K, Claassens J. An analytical solution for the inverse kinematics of a redundant 7 DOF Manipulator with link offsets. International Conference on intelligent Robots and Systems,2010:2976-2982.

[2] Punith K M, Sumanth S, Manikant A S. Internet Rescue Robots for Disaster Management. International Journal of Wireless and Microwave Technologies (IJWMT), 2021, 11(2): 13-23.

[3] Hussein M, Lotfi R, Mohammad A, et al. RRT*N: an efficient approach to path planning in 3D for Static and Dynamic Environments. Advanced Robotics, 2020, 35(3-4): 168-180.

[4] Angela S, Kane O. P, Virginia T, te al. The effect of intravenous dexamethasone on postoperative nausea and vomiting after Cesarean delivery with intrathecal morphine: a randomized-controlled trial Effet de la dexaméthasone intraveineuse sur les nausées et vomissements postopératoires après un accouchement par césarienne avec morphine intrathécale: un essai randomisé

contrôlé [J]. Canadian Journal of Anesthesia/Journal canadien d'anesthésie, 2020,67 (15): 1-15.

[5] Wen C Y, Huang C Q, Yang M, et al. The Secretion from Bone Marrow Mesenchymal Stem Cells Pretreated with Berberine Rescues Neurons with Oxidative Damage Through Activation of the Keap1-Nrf2-HO-1 Signaling Pathway [J]. Neurotoxicity Research: Neurodegeneration, Neuroregeneration, Neurotrophic Action, and Neuroprotection, 2020, 38(1): 1-14.

[6] Schneider H. Causal cognitive architecture 1: Integration of connectionist elements into a navigation-based framework. Cognitive Systems Research, 2021, 66: 67-81.

[7] Mattia S, Pratik S, Irina R, et al. Search and rescue at sea aided by hidden flow structures [J]. Nature Communications,2020,11(1):245-260.

[8] Junya T, Miki T, Ryo A, et al. Splicing- and demethylase-independent functions of LSD1 in zebrafish primitive hematopoiesis [J]. Scientific Reports, 2020,10(1):23-35.

[9] Kifayat U., Tahir M., Harish G.. Evaluation of the Performance of Search and Rescue Robots Using T-spherical Fuzzy Hamacher Aggregation Operators. International Journal of Fuzzy Systems, 2020, 22(1): 570-582.

[10] Tatsuya T., Masato M., Tomoaki H., et al. Development of the multifunctional rescue robot FUHGA2 and evaluation at the world robot summit 2018. Advanced Robotics, 2020, 34(2): 119-131.

[11] Miriam L, Kristian K. Ullrich, E, Diethard T. The amylase gene cluster in house mice (Mus musculus) was subject to repeated introgression including the rescue of a pseudogene [J]. BMC Evolutionary Biology, 2020,20(2):1-10.

[12] Michael S. F, Philip F. Stahel, J H, et al. Successful COVID-19 rescue therapy by extra-corporeal membrane oxygenation (ECMO) for respiratory failure: a case report[J]. Patient Safety in Surgery, 2020, 14(4): 1-15.

[13] Tetsushi K., Taichi A., Satoshi S., et al. Development of a separable search-and-rescue robot composed of a mobile robot and a snake robot. Advanced Robotics, 2020, 34(2): 132-139.

[14] Long X L., Xu Q W., Yuan Y J., et al. Improved Visual -Inertial Localization for Low-cost Rescue Robots. IFAC PapersOnLine, 2020, 53(2): 9709-9715.

[15] Takaya M., Wakaki U., Itaru N.. Development of a free viewpoint pedestrian recognition system using deep learning for multipurpose flying drone. Electronics and Communications in Japan, 2019, 102(11) : 16-24.